

Simulation of the dynamics of decompression sickness bubbles and the generation of new bubbles

H. D. VAN LIEW

Department of Physiology, University at Buffalo, SUNY, Buffalo, New York 14214

Van Liew HD. Simulation of the dynamics of decompression sickness bubbles and the generation of new bubbles. *Undersea Biomed Res* 1991; 18(4):333-345.—This communication introduces a system of equations for simulating the dynamics of growth and decay of decompression bubbles. The equations are solved by a numerical method and account for gas diffusion, the action of surface tension, tissue N_2 washout by blood, and the rate of ascent from depth. The simulations demonstrate how inward diffusion of N_2 can generate a persistent gas bubble from a nucleation process or a nucleus (these are provisionally defined as entities that can give rise to a small bubble of a certain size); an explosive positive-feedback loop is set off as the enlarging radius decreases the pressure due to surface tension. Generation of persistent bubbles is most likely during ascent from depth when PN_2 inside any gas phase is decreasing rapidly and PN_2 outside is still high before appreciable tissue washout has occurred. The "susceptibility" for the generation of a persistent bubble at any time can be defined as the reciprocal of the difference, at that time, between partial pressure of the nitrogen in tissue and in a spherical bubble of the size that is characteristic of the nucleation process or nucleus; susceptibility is less when ascent is slow because PN_2 in bubbles stays high while washout removes N_2 from the tissue.

ascent rate	gas nuclei
barotrauma	nucleation
bubble growth	oxygen window
bubble induction centers	surface tension
diving	susceptibility for generation of bubbles
	washout

Mathematical formulations for predicting behavior of gas bubbles provide an approach for studying the cause, prevention, and treatment of decompression sickness (DCS); decompression bubbles cannot be observed directly, except in highly structured experimental situations (1-3). Using mathematical treatments that are based on physical principles, various authors have been successful in characterizing bubble growth and decay in well-defined in vitro systems (4-7), but mathematical descriptions of phenomena that occur in living systems are by nature more approximate because of the many variables that are involved. Previous mathematical descriptions of DCS bubbles in animal tissues have been limited in one way or another.

Van Liew and Hlastala (8) did not account for surface tension, and Hlastala and Van Liew (9) investigated the role of transient phenomena but still left out surface tension effects. Kislyakov and Kopyltsov (10) simulated the generation of decompression bubbles from nuclei in an isolated region of tissue that could not exchange gas with nearby regions or blood, so the results were valid only for the very early stages of bubble growth. Meisel et al. (11) presented a more complete formulation but, as was the case for all the studies mentioned above, no provision was made for the gradual change of pressure during ascent from depth, so the results are strictly applicable only for bubbles after explosive decompression.

The major objective of this communication is to introduce a system of equations for predicting size of a bubble as a function of time. The system embodies seven commonly accepted concepts about decompression bubbles, which are listed below. Solutions are obtained by a numerical method. One major advantage of numerical methods is that mathematical complexities, non-linearities, and discontinuities can be handled; another is that it is relatively easy to incorporate new material into the system of equations if new information arises from research or new insights. Secondary objectives of this communication are to apply the equations to gain insight into how bubbles can arise, and to develop ideas about the susceptibility for persistent bubbles to be generated by a decompression.

ASSUMPTIONS AND EQUATIONS

The system of equations embodies the following concepts:

1. A gas bubble can be expected to increase in size in two circumstances—when there is a decrease of ambient pressure (expansion of gas according to Boyle's law) and when gas diffuses from the surroundings into the bubble. The inert gas dominates the diffusive exchanges since permeation of O_2 and CO_2 in and out of a gas phase are rapid (12).
2. Surface tension operates at gas/liquid interfaces; in a spherical bubble, surface tension causes pressure inside to exceed that outside by adding to the pressure on gas in the gas phase. Total pressure in a spherical bubble is the sum of the absolute gas pressure surrounding the body, pressure due to surface tension, pressure due to tissue elastic forces, and hydrostatic pressures due to body fluids and due to the water column if the body is immersed.
3. Living animal tissues have an intrinsic property that promotes absorption of gas bubbles. Called "inherent unsaturation" or "the oxygen window," this property is due to a deficit of oxygen partial pressure caused by oxygen consumption. The deficit is incompletely balanced by production of CO_2 , so partial pressure of inert gas in a bubble is greater than in the surrounding tissues and blood (12–14).
4. A simplistic interpretation of natural laws indicates that free spherical bubbles cannot be small because the oxygen window, abetted by surface tension, should cause bubbles to shrink until they cease to exist, but bubbles do occur in DCS. One way around this logical problem is to posit the existence of "gas nuclei" or "bubble formation centers," gaseous entities that either persist chronically or are generated occasionally (15–18); gas nuclei can be distinguished from real bubbles by their apparent failure to conform to expectations from the laws of

surface tension and diffusion for free spherical bubbles. Reasons for the failure could be that the nuclei are not free gaseous entities or not spherical. Alternatively, some sort of process, which can be called a "gas nucleation process," may focus energy in a way that generates gas bubbles (15).

5. When a person goes from one ambient-pressure environment to another, there is a readjustment of the inert gas dissolved in body fluids as gas "washes in" or "washes out." The washin or washout is relatively faster in tissues that have high perfusion with blood and in which solubility of the inert gas is low.
6. Small gas bubbles are spherical. Bigger bubbles are probably distorted into cylinders or sheets by tissue or blood vessels, but it seems logical that small bubbles are approximately spherical because of the strong effect of surface tension on them.
7. When a bubble grows, it tends to deplete the dissolved gas in its surroundings and when it shrinks, it supplies gas to its surroundings.

Equations

The simulations were developed with a MacIntosh IICx microcomputer in the BASIC programming language using the Euler method for numerical integration. All decompression simulations for this study were for air-breathing persons, and most were for decompression from 200 to 100 kPa (101.325 kPa = 760 torr = 1.0 atm = 33.08 fsw). The results of the simulations are presented with time, pressures, and radius as real, non-normalized values to facilitate insights into the phenomena being portrayed.

Definitions of symbols and values for constants appear in Table 1. The basic equation expresses the derivative (dR/dt) of radius with respect to time as

$$dR/dt = (\alpha_t \cdot D \cdot K_1) (1 - P_{tis_{N_2}}/P_{pub_{N_2}}) (\lambda + 1/R) \quad (1)$$

where

$$\lambda = [(\alpha_b \cdot K_2 \cdot \dot{Q})/(\alpha_t \cdot D)]^{0.5} \quad (2)$$

The derivation of Eq. 1 appears in Van Liew and Hlastala (8). Major assumptions for the present use of the equation are that it contains all the important variables for describing gas bubbles and that the equation can be integrated by a numerical method when all the variables are subject to change. If tissue washout is limited by perfusion alone, the value of K_2 in Eq. 2 is 1.0; setting its value to less than 1 allows the simulation of diffusion limitation.

Several of the seven main items in Eq. 1 are functions of the equations that follow. The calculation process is to solve each equation, 1 through 7, for a small time increment using chosen initial values for the variables, integrate Eqs. 1, 4, and 6 by adding the differential values to the previous values of the variables, then solve each equation again using the newly calculated values for the variables, and so on. Duration of the time increments were usually 12 s, chosen to give a solution which did not change when duration of the increment was decreased.

The value of $P_{tis_{N_2}}$ is defined in terms of volume of gas dissolved in a unit of tissue; this volume changes as gas is washed in or out by the blood supply.

TABLE 1
DEFINITIONS OF SYMBOLS AND VALUES FOR CONSTANTS

Constants

D	= diffusivity of N_2 in body fluids, $0.00132 \text{ cm}^2 \cdot \text{min}^{-1}$
FI_{O_2}	= fraction of O_2 in inspired gas, 0.21 (dimensionless)
K_1	= constant, 100 kPa
K_2	= constant for effectiveness of blood flow, 1.0 (dimensionless—setting the value of K_2 to less than 1.0 allows for simulation of diffusion limitation)
K_3	= conversion factor, $10,000 \text{ dyn} \cdot \text{cm}^{-2} \cdot \text{kPa}^{-1}$
PA_{CO_2}	= partial pressure of CO_2 in alveolar gas, 5.3 kPa
P_{H_2O}	= partial pressure of water vapor, 6.2 kPa
P_{tisCO_2}	= partial pressure of CO_2 in tissue, 5.9 kPa
P_{tisO_2}	= partial pressure of O_2 in tissue, 5.3 kPa
α_b	= solubility of N_2 in blood, $0.000144 (\text{ml}_{\text{STPD}}/\text{ml}) \cdot \text{kPa}^{-1}$
γ	= surface tension, 50 dyn/cm

Variables

A	= ascent rate, $\text{kPa} \cdot \text{min}^{-1}$
P_{tisN_2}	= partial pressure of dissolved N_2 in tissue, kPa
P_{tisN_2}'	= partial pressure of dissolved N_2 in tissue after equilibration at a certain P_B , kPa
P_B	= ambient pressure at a particular time, kPa
P_{bubN_2}	= partial pressure of N_2 in a bubble, kPa
\dot{Q}	= tissue perfusion rate, $\text{ml} \cdot \text{ml}^{-1} \cdot \text{min}^{-1}$
R	= radius, cm
t	= time, min
v	= tissue volume, ml
V	= bubble volume, ml_{ATPS}
V_t	= volume of N_2 in the tissue volume, ml_{STPD}
α_t	= solubility of N_2 in tissue, 1 to 5 times α_b
λ	= a constant for any particular bubble, defined by Eq. 2

$$P_{tisN_2} = V_t / (\alpha_t \cdot v) \quad (3)$$

$$dV_t/dt = \alpha_b \cdot \dot{Q} \cdot v \cdot (P_{tisN_2} - P_{tisN_2}') + P_{bubN_2} \cdot dV/dt \quad (4)$$

where the value of V is obtained from the integration of Eq. 1 plus the formula for volume of a sphere, $V = 4 \cdot \pi \cdot R^3/3$. The first term in Eq. 4 allows for exponential decay of N_2 as washout occurs and the second modifies the washout by amounts of N_2 that are taken from the tissue by growth of the bubble. *Note* that \dot{Q} appears in both Eqs. 2 and 4. The value of P_{tisN_2}' , the endpoint toward which washin or washout approaches, is a function of barometric pressure at any time

$$P_{tisN_2}' = P_B - F_{I_{O_2}} \cdot P_B - P_{ACO_2} - P_{H_2O} \quad (5)$$

Barometric pressure changes during ascent

$$dP_B/dt = A \quad (6)$$

The value P_{bubN_2} of Eq. 1 is affected by other gases in the bubble and by total pressure in the bubble, which is determined by barometric pressure and pressure due to surface tension

$$P_{bubN_2} = P_B - (P_{tisO_2} + P_{tisCO_2} + P_{H_2O}) + 2 \cdot \gamma / (R \cdot K_3) \quad (7)$$

The radius of the bubble affects radius change in three ways: by the geometry effect in Eq. 1, by depletion of gas from the tissue around the bubble in Eq. 4, and by the surface tension effect in Eq. 7. Both the geometry component and the surface tension component of the radius change are functions of the reciprocal of radius, so the radius of a small bubble changes rapidly, be it to grow or to shrink.

Nucleation and nuclei

I arbitrarily define nucleation processes and nuclei as processes or entities that can give rise to unstable spherical gas bubbles of a specified size. This provisional definition of nucleation processes and nuclei seems as good as any other given the present state of knowledge (15). The quintessence of the definition is the specification of the size of the newly generated bubble for a particular nucleus or nucleation process. Once a bubble is generated, it is assumed that it is governed by the equations in all respects, and some new bubbles will be reabsorbed immediately; bubbles that do not grow enough to persist for at least a few minutes are not of concern here. It is implicit in what follows that new bubbles can be generated at any time; this seems reasonable for nuclei but may not be the case for a nucleation process, which may depend on an external event such as a movement of the body or the penetration of a cosmic ray.

RESULTS

In Fig. 1A, ambient pressure (P_B , broken line) and partial pressures of N_2 are plotted as functions of time. During the ascent, ambient pressure goes from 200 to

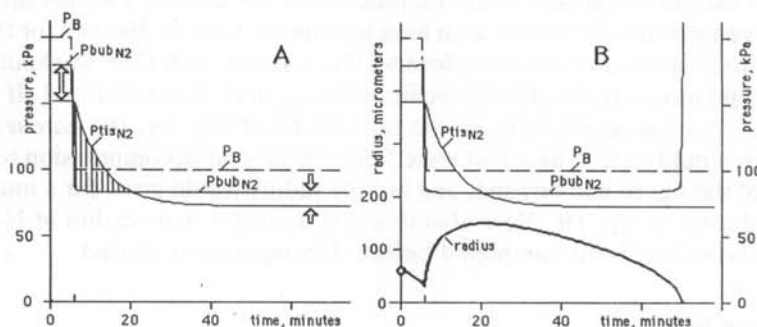


Fig. 1. Simulations of pressure profiles and radius changes of a preexisting bubble at the time of a decompression from 200 kPa (2 atm) to the surface. A, ambient pressure (broken line) and partial pressures of N_2 in a preexisting bubble and in the surrounding tissue; B, same as A, with radius of the bubble added.

100 kPa at a rate of $200 \text{ kPa} \cdot \text{min}^{-1}$, close to the standard ascent rate for U.S. Navy diving tables ($60 \text{ fsw} \cdot \text{min}^{-1} = 184 \text{ kPa} \cdot \text{min}^{-1}$); on the time scale of the diagram, the fall of P_B seems to be almost instantaneous. Consider a bubble that is large enough that pressure due to surface tension is negligible. When ambient pressure falls, partial pressure of N_2 inside the bubble ($P_{\text{bub}_{N_2}}$) falls too. For the present treatment, elastic recoil of the tissue is considered negligible, so the sum of partial pressures inside the bubble equals ambient pressure; the P_{N_2} inside is always a little lower than ambient pressure because the bubble contains O_2 , CO_2 , and water vapor as well as N_2 . The sum of tissue O_2 and CO_2 is relatively constant over a range of ambient pressures in air-breathing persons, so the difference between P_B and $P_{\text{bub}_{N_2}}$ is about the same when P_B is 200 kPa (Fig. 1A, *left*), or 100 kPa (Fig. 1A, *right*). For the case shown, $P_{\text{bub}_{N_2}}$ is about 20 kPa less than P_B .

The *vertical hatching* in Fig. 1A shows what can be called a "crossover," where partial pressure of N_2 in the tissue ($P_{\text{tis}_{N_2}}$) is temporarily higher than partial pressure of N_2 in the bubble; tissue N_2 must await washout by the circulation. In steady states, $P_{\text{tis}_{N_2}}$ is below $P_{\text{bub}_{N_2}}$; Fig. 1A, *arrows*, show the magnitude of the driving pressure for bubble absorption (the oxygen window) in the two steady states; when $P_B = 200 \text{ kPa}$, it is 36 kPa and when $P_B = 100 \text{ kPa}$ it is 9 kPa.

Figure 1B shows the calculated radius of a preexisting bubble (arbitrarily given a radius of $60 \mu\text{m}$, presumably well above the size that would be generated anew) when it is subjected to the decompression discussed in Fig. 1A. At first the bubble shrinks to $30 \mu\text{m}$ due to the oxygen window. If the ascent had been just a minute or so later the bubble would have ceased to exist. When the ascent occurs, the bubble enlarges because of decompression of the gas (Boyle's law), but there is also a crossover of N_2 , so the bubble grows by inward diffusion of N_2 molecules. The Boyle's law effect alone would have increased the bubble from 30 to $38 \mu\text{m}$, whereas it actually grows to $150 \mu\text{m}$. When tissue P_{N_2} becomes lower than bubble P_{N_2} (after 20 min), the bubble shrinks again. When the radius becomes very small, at 70 min, surface tension causes a precipitous rise in $P_{\text{bub}_{N_2}}$, seen as an almost vertical trace (Fig. 1B, *right*).

For illustrative purposes, the figures of this communication have been drawn for tissues in which dissolved N_2 washes out quite rapidly, but a broader perspective can be reached if it is remembered that bubbles or nuclei in the body may be in contact with tissues with different washout characteristics than are shown in the specific examples given here. The time frame for tissue washout in Fig. 1 (5 min half-time) is an order of magnitude greater than the time frame for ascent, and this discrepancy would be even greater for tissues with long half-times, such as 360 min for the tissues of concern to aviators and space explorers (19). A tissue with slow washout, a "slow tissue," would have a much slower decline of $P_{\text{tis}_{N_2}}$ than shown in Fig. 1. If the $P_{\text{tis}_{N_2}}$ trace did not decline appreciably in the time frame of Fig. 1A, the *hatched bubble-growth area* would extend as a rectangle from the time of decompression toward the *right side* of the figure and beyond, and bubble radius would grow for a much longer time than shown in Fig. 1B. *Note* also that it is assumed that washin of N_2 into this particular tissue had been completed before decompression started.

Generation of bubbles

Figure 2A illustrates the generation of a bubble for the same decompression as in Fig. 1. A large bubble in which the effect of surface tension is negligible would have

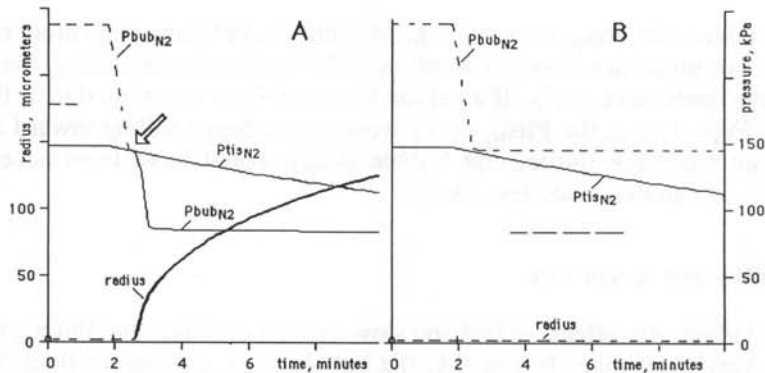


Fig. 2. A, simulation of the generation of a new gas bubble for the same pressure profile as in Fig. 1 (the P_B trace is left out for clarity). Dashed parts of the $P_{\text{sub}N_2}$ and radius traces in Figs. 2 and 3 indicate characteristics of the bubble that could be generated by a particular nucleus or nucleation process; after the bubble is generated, the traces are solid. B, in a potential bubble that is slightly smaller than the one in A, the $P_{\text{sub}N_2}$ is high due to surface tension so that a crossover is avoided and no growth occurs.

a P_{N_2} inside of about 180 kPa (Fig. 2A, broken line, extreme left), whereas the bubble of the size that will be generated by the particular nucleation process or nucleus that was chosen for this case would have a $P_{\text{sub}N_2}$ of almost 240 kPa as shown—the difference is due to the high pressure caused by surface tension consequent to the 1.58- μm radius that was chosen. A tiny crossover at the arrow allows the new bubble to grow very slightly—too small a growth to show immediately on the radius trace. After a lag period of very slow growth that lasts less than half a minute, there is a rapid decrease of surface tension pressure so that P_{N_2} inside the bubble falls (from the level of the arrow to 90 kPa). The nature of the lag will be taken up in the Discussion.

When size of the bubble that can be generated is just one one-hundredth of a micrometer smaller, a different picture emerges (Fig. 2B). The starting value of $P_{\text{sub}N_2}$ is slightly higher than in Fig. 2A because the smaller radius of the newly generated bubble causes a higher surface tension pressure, and after ascent the $P_{\text{sub}N_2}$ is about 150 kPa whereas a large bubble would have a P_{N_2} of about 90 kPa (Fig. 2B, broken line). Although $P_{\text{sub}N_2}$ comes close to $P_{\text{tis}N_2}$ at the end of the ascent, there is never a crossover so there is no sustained growth phase, even though a gaseous entity would have had a small Boyle's law enlargement during the decompression.

Note that the bubble sizes chosen for Fig. 2A, B were arbitrary. There probably is a range of sizes of gaseous nuclei in tissues (17) or of sizes generated by nucleation processes; if so, one might envision a family of parallel $P_{\text{sub}N_2}$ traces on Fig. 2, with the larger sizes of potential bubbles giving rise to lower traces. To gain generality from a single $P_{\text{sub}N_2}$ trace, one can conceive of the "susceptibility" for a crossover to occur; without a crossover there is no possibility for a persistent bubble to form. Susceptibility can be defined as the reciprocal of the difference between $P_{\text{sub}N_2}$ and $P_{\text{tis}N_2}$; in Fig. 2B the susceptibility is maximal at 2.5 min. Even if the trace of a particular nucleation process or nucleus does not exhibit a crossover, other parallel traces may.

Several variables can be critical for the generation of a bubble. One of these is size of the unstable bubble that is generated, as seen above. Also, if the tissue washout

had been faster, the P_{tisN_2} curve of Fig. 2A would have fallen away more rapidly and the crossover might not have occurred, or if the washout were slower, the crossover would have been more likely. If a person breathed O_2 at any time during the profiles shown in Figs. 1 or 2, the P_{tisN_2} curve would have begun falling toward zero as N_2 washed out from the tissue, and bubble decay would have been accelerated or generation of bubbles made less likely.

Susceptibility and ascent rate

Figure 3 illustrates effects of fast and slow ascents on P_{tisN_2} and P_{bubN_2} for a tissue having a 5-min half-time. In Fig. 3A, the bubble sizes are smaller than in Fig. 2 so the P_{bubN_2} traces are higher (*broken lines*). When ascent is at the standard rate (*light traces*), the N_2 washout from tissue assumes the expected exponential form but with the slower ascent ($5 \text{ kPa} \cdot \text{min}^{-1}$, *dark traces*), the P_{tisN_2} tends to follow almost in parallel to the P_{bubN_2} , which of course is following the slow fall of ambient pressure. The susceptibility for generation of a bubble is less for the slow ascent because the minimal vertical distance between the *light traces* is only about 20 kPa at 4 min compared to 70 kPa or more for the *heavy traces*.

Figure 3B illustrates the susceptibility for bubbles to form when a tissue with given tissue washout characteristics is subjected to different ascent rates. A 10-fold decrease of ascent rate extends the time when the tissue has lost half its N_2 by about 3 min, and decreases the susceptibility by a factor of 2 as shown by *black arrows*. One could conclude from this comparison that the high P_{N_2} in the gas phase during the slow ascent is more of an advantage than the somewhat faster washout with the fast ascent. Only very slow ascent has an appreciable effect on removal of N_2 from tissue. When ascent is decreased 40-fold from the standard $200 \text{ kPa} \cdot \text{min}^{-1}$, the slower ascent causes a large decrease in the susceptibility for bubble generation, shown in Fig. 3B (*dark arrow, right*), and the removal of N_2 is delayed so that the tissue loses half its excess N_2 in about 20 min.

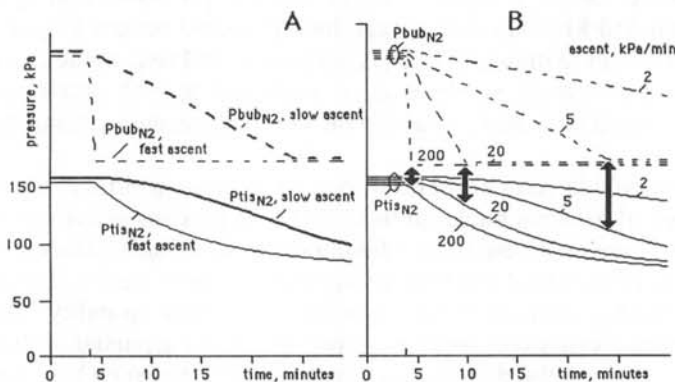


Fig. 3. Effect of ascent rate on the tendency for generation of persistent bubbles from nucleation processes or nuclei. Traces for different ascents are offset slightly for clarity. A, the P_{tisN_2} and P_{bubN_2} in a slow ascent (*heavy traces*) are compared with N_2 pressures in the standard ascent rate of $200 \text{ kPa} \cdot \text{min}^{-1}$. B, arrows show susceptibilities for bubble generation for a range of different ascent rates; long arrow signifies low susceptibility.

Simulations that compared a 200 kPa to a 100 kPa decompression with decompressions having the same ratio (from 400 to 200 kPa or 800–400 kPa) showed that the growing bubbles reached approximately the same size; the breathing gas was air for all cases and the small differences in size reached are traceable to small differences in the O_2 window and time of crossover. The finding has a physical basis: twice as many gas molecules enter the bubble in the 400:200 decompression as in a 200:100 decompression, but it takes twice as many molecules to make a volume and radius of a given size at 200 kPa as at 100 kPa.

Although the growing bubbles reached the same size when different 2:1 decompression ratios were tested, the minimal radius of the newly generated bubbles was found to be inversely related to total pressure. For example, the minimal radius that can give rise to a bubble for an 800:400 decompression was about half the minimal radius for a 200:100 decompression. The minimal radius is probably highly sensitive to the assumptions about very small bubbles; more sophisticated assumptions may yield a different picture. If the finding about minimal radius is valid, it means that a larger number of bubbles can be expected at an 800–400 kPa decompression because, in addition to nucleation processes or nuclei that generated bubbles when decompression was from 200 to 100 kPa, processes or nuclei that can give rise to smaller bubbles will also be productive.

DISCUSSION

The simulations indicate that the generation of spherical bubbles involves a positive feedback loop, so the process tends to be an all-or-none phenomenon. In Fig. 2A, a fall of total pressure causes an infinitesimal crossover to occur, meaning that P_{bubN_2} becomes less than P_{tisN_2} (Fig. 4, box 1). During the short lag period in Fig. 2A, N_2 that diffuses into the gas phase (Fig. 4, box 2) depletes the dissolved gas in the tissue, tending to lower the diffusion gradient; there is competition between gas phase and surroundings for N_2 as long as the surface forces keep a high total pressure inside the gas phase. If some influence during the short lag period had decreased the tendency for growth, the positive feedback action might be aborted, but once the gas phase starts to grow appreciably, the rapid fall of pressure due to surface tension

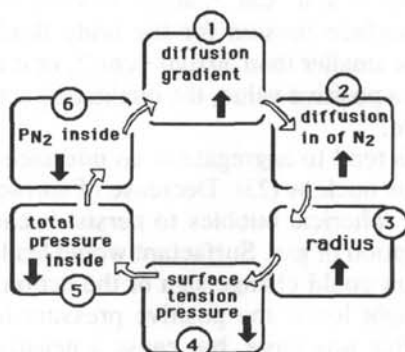


Fig. 4. The positive feedback loop that is involved in generation of persistent bubbles from nucleation processes or nuclei.

ensures that the process will proceed. Once enough gas has diffused in to increase the radius slightly (Fig. 4, *box 3*), pressure due to surface tension falls (*box 4*), total pressure falls (*box 5*) with consequent fall of P_{N_2} (*box 6*) and increase of the diffusion gradient (*box 1*), thus continuing the self-propagating feedback. Almost immediately, the total pressure in the gas phase (*box 5*) is well below that in the tissue, so competition between gas phase and tissue for N_2 becomes negligible unless the bubble becomes so large that it contains most of the excess N_2 that was originally in the tissue. The positive feedback loop will stop its action when the radius is large enough that changes of surface tension pressure (*box 4*) no longer contribute importantly to total pressure inside the gas phase.

Some cases in which the loop's action could be initiated at sites other than in Fig. 4, *box 1* come to mind: metabolically produced CO_2 , a different breathing gas such as He, an anesthetic gas such as nitrous oxide, or some other gas could enter the gas phase. This would have two effects: The presence of the other gas would lower P_{N_2} inside (Fig. 4, *box 6*) with consequent inward diffusion of N_2 , and the added volume of the other gas would increase the radius (*box 3*) with consequent decrease of surface tension pressure. Such a mechanism probably underlies isobaric bubble-formation phenomena (20, 21). Another possibility could be some sort of physical influence which would temporarily increase the radius of the gas phase (Fig. 4, *box 3*). A small isolated increase of radius might not activate the loop if the amount of N_2 added by inward diffusion were lost again by prevailing conditions that caused outward diffusion, but if the stress were large it might cause enough diffusion to start the loop action. Presumably in tribonucleation (22) a physical disturbance either creates a gas phase or enlarges a gas phase that is associated with an existing nucleus, and enough gas accumulates by diffusion to start the feedback loop. Also, a series of small perturbations, such as vibration, might have a cumulative effect that could start the loop; if there is not time between pulses for outward diffusion of all that entered, the accumulation of gas could start the loop.

Surface tension

Surface tension plays a pivotal role in the feedback loop. The pressure exerted by interfacial tension acts to prevent growth, but once growth occurs, the sharp fall of surface forces engenders further growth. For the simulations, I arbitrarily used a value for surface tension of $50 \text{ dyn} \cdot \text{cm}^{-1}$, about 70% the value of $72 \text{ dyn} \cdot \text{cm}^{-1}$ for water. The appropriate surface tension for the body fluids in which bubbles are generated may be larger or smaller than $50 \text{ dyn} \cdot \text{cm}^{-1}$, or it may be variable. As long as the surface tension has a positive value, the qualitative action of the feedback loop will be as described above.

Surface-active materials tend to aggregate at an interface between gas and liquid, be it a bubble or a gaseous nucleus (23). Decrease of surface tension to zero would not be expected to allow spherical bubbles to persist because the oxygen window would still promote absorption of gas. Surfactant would lead to a persistent gas-filled nucleus only if a surfactant could change sign of the action of surface tension. The presence of surfactant might lower the positive pressure inside the bubble due to surface tension if the radius was large, but cause a negative pressure inside if the radius became very small, perhaps by interaction with a structure in which the nucleus is located; a "crevice" is one possibility for such a structure (24). Negative pressure

would tend to lower P_{N_2} inside and would thus promote inward diffusion of N_2 to counter the tendency for outward diffusion due to the oxygen window. It could be that surfaces of nuclei are lined by materials that are similar to the special surfactant that is found on the alveolar surfaces of the lung; pulmonary surfactants cause surface tension to increase when the area of the gas phase grows, thus inhibiting growth, and decrease when the area shrinks, inhibiting the shrinkage. Presumably, once the radius of curvature is large, the effect of surface tension is no longer important, but surfactant molecules may alter the permeability of the bubble/tissue interface.

Susceptibility and ascent rate

The susceptibility for the all-or-none growth to produce bubbles can be predicted from the nearness of the profiles of $P_{bub_{N_2}}$ and $P_{tis_{N_2}}$, as in Figs. 3 and 4. A newly generated bubble that has a large radius has the lowest partial pressure of N_2 inside the bubble, so it will be most susceptible during a particular decompression. The more stressful the decompression, say 250–100 instead of 200–100, the smaller the difference between $P_{bub_{N_2}}$ and $P_{tis_{N_2}}$ because of high $P_{tis_{N_2}}$, so some processes or nuclei that generate small-radius bubbles will be productive in addition to those that generate large-radius ones.

After ascent, $P_{tis_{N_2}}$ falls away due to inert gas washout from tissues, widening the distance between $P_{bub_{N_2}}$ and $P_{tis_{N_2}}$, so susceptibility for generation of bubbles tends to be highest at the time of ascent. The implication that all bubbles are generated during ascent contrasts with the observation that signs and symptoms of DCS commonly arise minutes or hours after ascent (18, 25). Perhaps during this latent period, bubbles which had formed during the ascent have grown larger in the sites where damage occurs, or migrated to the sites from elsewhere. One can conceive of exceptions to the idea that bubbles are generated only at the time of ascent: A nucleus which did not generate bubbles during ascent could migrate to N_2 -rich environments at some later time, or nuclei could be activated late if gas diffuses into a region and makes a late crossover. If nuclei are continuously being formed anew or if nucleation processes occur at random times, bubbles could be generated after the ascent but before the crossover has decayed.

Slow ascents tend to decrease the susceptibility because they keep total pressure in gas bubbles high even though they slow the removal of N_2 from the tissues (Fig. 3). The tissue at risk for any decompression depends on whether the bottom time has resulted in a large N_2 load in fast tissues only (short bottom time), all tissues (long bottom time = saturation), or fast and intermediate tissues only (intermediate bottom time). When ascent occurs while the tissues are still taking up inert gas, tissues with slow and intermediate washin rates can take up additional gas during a slow ascent; this may make the intermediate tissues most susceptible to generation of bubbles. Tissues with very long washout half-times would benefit from slow ascents only if the ascents were similar in duration to the half-times.

A way of gaining an advantage that is similar to a slow ascent is to stop a regular ascent at a depth near the surface for a short time, a so-called "safety stop." The effect on susceptibility can be visualized by reference to Fig. 2. The $P_{bub_{N_2}}$ would have a period of pause a little above the level it finally attains, and during that time the $P_{tis_{N_2}}$ would become low enough that a crossover would be avoided when the

final ascent to the surface occurs. This procedure should cut down on the number of bubbles because only large, newly generated bubbles could have a crossover.

Validity of assumptions and application to decompression sickness

The conclusions that arise from a computer simulation depend completely on the assumptions that are embodied in the equations. Where growth and decay of sizable bubbles are concerned, the validity of the system of equations used for this communication can be established by comparison of simulation results with experimental data from observations of bubbles. My equations give satisfactory correspondence with published data from large subcutaneous gas pockets (26), air bubbles in water (6, 27), and bubbles in adipose tissue (3). Actually, the behavior of these observed cases can be approximated quite well even with mathematical treatments that do not provide for the complexities of living tissue, such as the treatment of Epstein and Plesset (4).

No system of equations can be expected to reflect all the complexity of a natural phenomenon; the inferences reached above about newly generated small bubbles are only valid if the assumptions are appropriate. The definition of nucleation processes and nuclei used here does not ascribe any characteristics to the process or nucleus; the definition is concerned only with the size of the bubble at the precise time that it is generated. The validity of the system of equations can be questioned in the very realm in which the simulations are most interesting: with very small bubbles. Such matters as transient effects involving the gas dissolved in the tissue immediately adjacent to the gas phase and convective influence of movement of the gas/tissue boundary can be expected to increase in influence as bubble size decreases. More sophisticated mathematical treatments may shed light on the weaknesses of the equations for very small gas quantities. Also, initial steps in the generation of bubbles may be complex; for example, a gaseous nucleus in a hydrophobic crevice (24) would undergo a pressure transient as the gas in the nucleus enlarges; curvature of the gas/liquid interface is expected to change sign when the enlarging nucleus reaches the crevice opening and then a bud developing outside the crevice goes through a phase of increasing surface tension pressure before breaking off as a bubble, in which further enlargement means decrease of surface tension pressure. In any case however, persistent bubbles cannot develop unless a crossover of $P_{tis_{N_2}}$ and $P_{bub_{N_2}}$ occurs; the simulations presented above demonstrate the importance of the interplay between nitrogen diffusion into the gas phase and pressure due to surface tension.

The author expresses profound appreciation to J. Conkin, M. P. Hlastala, B. E. Shykoff, and R. D. Vann for encouragement and very helpful suggestions.—*Manuscript received June 1990; accepted May 1991.*

REFERENCES

1. Daniels S, Paton WDM, Smith EB. Ultrasonic imaging system for the study of decompression-induced gas bubbles. *Undersea Biomed Res* 1979; 6:197-207.
2. Lynch PR, Brigham M, Tuma R, Wiedeman MP. Origin and time course of gas bubbles following rapid decompression in the hamster. *Undersea Biomed Res* 1985; 12:105-114.
3. Hyldegaard O, Madsen J. Influence of heliox, oxygen, and N_2O-O_2 breathing on N_2 bubbles in adipose tissue. *Undersea Biomed Res* 1989; 16:185-193.
4. Epstein PS, Plesset MS. On the stability of gas bubbles in liquid-gas solutions. *J Chem Physics* 1950; 18:1505-1509.

5. Tikuisis P, Ward CA, Venter RD. Bubble evolution in a stirred volume of liquid closed to mass transport. *J Appl Physics* 1983; 54:1-9.
6. Wyman J, Scholander PF, Edwards GA, Irving L. On the stability of gas bubbles in sea water. *Sears Foundation J Marine Res* 1952; 11:47-62.
7. Yang WJ. Dynamics of gas bubbles in whole blood and plasma. *J Biomech* 1971; 4:119-125.
8. Van Liew HD, Hlastala MP. Influence of bubble size and blood perfusion on absorption of gas bubbles in tissues. *Respir Physiol* 1969; 7:111-121.
9. Hlastala MP, Van Liew HD. Absorption of in vivo inert gas bubbles. *Respir Physiol* 1975; 24:147-158.
10. Kislyakov YY, Kopyltsov AV. The rate of gas-bubble growth in tissue under decompression. Mathematical modelling. *Respir Physiol* 1988; 71:299-306.
11. Meisel S, Nir A, Kerem D. Bubble dynamics in perfused tissue undergoing decompression. *Respir Physiol* 1981; 43:89-98.
12. Van Liew HD, Bishop B, Walder-D P, Rahn H. Effects of compression on composition and absorption of tissue gas pockets. *J Appl Physiol* 1965; 20:927-933.
13. Lategola MT. Measurement of total pressure of dissolved gas in mammalian tissue in vivo. *J Appl Physiol* 1964; 19:322-324.
14. Hills BA. Decompression sickness. The biophysical basis of prevention and treatment. New York: John Wiley & Sons, 1977:239-243.
15. Hemmingsen EA. Nucleation of bubbles in vitro and in vivo. In: Brubakk AO, Hemmingsen BB, Sundnes G, eds. Supersaturation and bubble formation in fluids and organisms. Trondheim, Norway: Tapir Publishers, 1989:43-59.
16. Vann RD, Grimstad J, Nielsen CH. Evidence for gas nuclei in decompressed rats. *Undersea Biomed Res* 1980; 7:107-112.
17. Strauss RH. Bubble formation in gelatin: implications for prevention of decompression sickness. *Undersea Biomed Res.* 1974; 1:169-174.
18. McDonough PM, Hemmingsen EA. A direct test for the survival of gaseous nuclei in vivo. *Aviat Space Environ Med* 1985; 56:54-56.
19. Waligora JM, Horrigan DJ, Conkin J. The effect of extended O₂ prebreathing on altitude decompression sickness and venous gas bubbles. *Aviat Space Environ Med* 1987; 58:A110-A112.
20. D'Aoust BG, Smith KH, Swanson HT, et al. Venous gas bubbles: production by transient, deep isobaric counterdiffusion of helium against nitrogen. *Science* 1977; 197:899.
21. Graves DJ, Idicula J, Lambertsen CJ, Quinn JA. Bubble formation in physical and biological systems: a manifestation of counterdiffusion in composite media. *Science* 1973; 179:582-584.
22. Ikels KG. Production of gas bubbles in fluids by tribonucleation. *J Appl Physiol* 1970; 28:524-527.
23. Yount DE, Kunkle TD, D'Arrigo JS, Ingle FW, Yeung CM, Beckman EL. Stabilization of gas cavitation nuclei by surface active compounds. *Aviat Space Environ Med* 1977; 48:185-191.
24. Tikuisis P. Modeling the observations of in vivo bubble formation with hydrophobic crevices. *Undersea Biomed Res* 1986; 13:165-180.
25. Eckenhoff RG, Parker JW. Latency in onset of decompression sickness on direct ascent from air saturation. *J Appl Physiol* 1984; 56:1070-1075.
26. Van Liew HD, Schoenfisch WH, Olszowka AJ. Exchanges of N₂ between a gas pocket and tissue in a hyperbaric environment. *Respir Physiol* 1968/1969; 6:23-28.
27. Buckles RG. The physics of bubble formation and growth. *Aerosol Med* 1968; 39:1062-1069.